Synthesis Emission Spectra of (LIPS) Technique for Cu, Ag Nanoparticles and their Antibacterial Activity

Hadeel K. Nasif[1], Baida M. Ahmed[1*], Kadhim A. Aadim[2]

[1] Department of Physics College of Science, Mustansiriyah University, Baghdad, IRAQ.
[2] Department of Physics College of Science, Baghdad University, Baghdad, IRAQ.

*Correspondent email: dr.baida_222@uomustansiriyah.edu.iq

ABSTRACT

A spectroscope presents the optical emission spectroscopy (OES) technique on laser-produced copper and silver plasmas. The optical emission spectrum technique was used to analyzes the spectrum arising from the Cu, Ag Laser Nd: YAG plasmas with a wavelength of (1064) nm, a span of (10) ns, and a focal length of (10) cm in the energy range (300-800) mJ. The electron temperature (T_e) was determined while the Saha-Boltzmann equation was used to measure the electron density (n_e). Other plasma parameters, (λ_D), (f_p), (N_D), were also measured. For various energies, the plasma spectrum was registered copper and silver. Q-switched Nd: YAG liquid laser ablation technique (PLAL) was used to produce nanoparticles (NPs), silver, and copper particles using distilled water at room temperature at different energies (300-600-800) mJ. With a constant wavelength (1064nm). At a constant frequency ($6H_z$), 300 laser pulses were used to ablate the target placed in distilled water to study the effect of these materials in inhibiting bacteria. Bacteria were used (Staphylococcus). This study showed that (Ag-NPs) and (Cu-NPs) that are synthesized by laser ablation have a great effect on Staphylococcus (antibiotic-resistant) bacteria.

KEYWORDS: Spectroscopy; LIBS; PLAL; plasma parameters; Silver; Copper.

الخلاصـة

تقنية التحليل الطيفي الانبعاثات الضوئية (OES) على بلازما النحاس والفضة المنتجة بالليزر. تم استخدام تقنية طيف الانبعاث البصري لتحليل الطيف الناتج عن البلازما Ag,Cu للليزر Nd: YAG بطول موجة (1064) نانومتر و امتداد (10) نانوثانية بطول بؤري (10) سم ضمن مدى الطاقة (800-300) مللي جول. تم تحديد درجة حرارة الإلكترون (Te) بينما تم استخدام معادلة Saha-Boltzmann لقياس كثافة الإلكترون (ne). تم أيضًا قياس معلمات البلازما الأخرى (λ_D) ,(f_p), (N_D). بالنسبة للطاقات المختلفة ، تم تسجيل طيف البلازما من النحاس والفضة. تم استخدام تقنية Qswitched Nd: YAG الليزر السائل (PLAL). لإنتاج الجسيمات النانوية (NPs) والفضة والنحاس باستخدام الماء المقطر في درجة حرارة الغرفة وبطاقات مختلفة (800-600-300) مللي جول. بطول موجة ثابت (1064 نانومتر). على تردد ثابت (6 هرتز) ، تم استخدام 300 نبضة ليزر لاجتثاث الهدف الموضوع في الماء المقطر لدراسة تأثير هذه المواد في تثبيط البكتيريا. تم استخدام البكتيريا (المكورات العنقودية). أظهرت هذه الدراسة أن (Ag-NPs) و (Cu-NPs) اللذين يتم تصنيعهما عن طريق الاستئصال بالليزر لهما تأثير كبير على بكتيريا Staphylococcus (المقاومة للمضادات الحيوية).

INTRODUCTION

Laser-Induced Breakdown Spectroscopy [LIBS] is a standard method for promoting detailed quantitative physical analysis in situ. As the excitation source, it utilizes a high-energy laser pulse. It can be used to analyze any material, such as gas, solid, or liquid, regardless of its physical state with the help of its laser-induced plasma emission signals{Hanif, 2014 #275}, it tracks those atomic and molecular species[1].{Hanif, 2014 #275}{Hanif, 2014 #275}

This operates on the surface of the target material with the laser beam and generates the plasma. In this process, the laser beam excites and ionizes the target material. The plasma emission will begin on the target surface of the material as soon as the laser photon hits the target surface. The laser-induced plasma emission spectra can detect atomic and molecular species for optical application. The set of experimental conditions influences LIBS analytical outcomes. LIBS performance is influenced by laser pulse energy, pulse rate, observation time rate, atmospheric gas pressure, target form, properties of the target material, geometric structure of optical instruments [2, 3].

The important influence on optical emission spectroscopy is seen by Laser-Induced Plasma

(LIP). The dominant technique to generate the plasma electronically from the plasma aroused species is considered [4]. The optical radiation spectrum using the ratio theory is one of the features of the LIPS essentially; it is used to measure electron temperature and density. In this process, the energies of the electrons are distinguished [5]. The thermodynamic equilibrium equation describes the plasma temperature with Local Thermal Equilibrium (LTE)[6].

$$T = \frac{-(E_1 - E_2)}{k \, ln\left(\frac{I_1 \lambda_1 A_2 g_2}{I_2 \lambda_2 A_1 g_1}\right)} \qquad (1)$$

(Eq. 1) the intensity is referred to by l_1, l_2, and g_1, g_2 as the statistical weight. A_1, A_2 is referred to as the probability of transition. λ_1, λ_2 is a wavelength. E_1 and E_2 are referred to as the excited state energy values in eV, K_B is representing the Boltzmann constant. The number of free electrons per unit volume is determined by the electron density. The equation is developed from the principles of Boltzmann Saha, spectral lines of the same element and successive stages of ionization [7].

$$n_e = \frac{I_1}{I_2^*} 6.04 \times 10^{21} (T)^{3/2} e^{\frac{(E_1 - E_2 - X_z)}{K_B T}} \qquad (2)$$

(Eq. 2) X_z is the ionizing energy in eV, n_e is the density of electrons. E_1 and E_2 are referred to as the excited state energy values in eV. K_B is representing the Boltzmann Continuous.

$$I_2^* = \frac{I_2 \lambda_2}{g_2 A_2} \qquad (3)$$

(Eq. 3) g_2, λ_2 and A_2 represent the transition from level2. The plasma frequency can be obtained from the following equation [8].

$$f_p = \sqrt{\frac{e^2 \, n_e}{m_e \, \varepsilon_o}} \qquad (4)$$

(Eq. 4) The frequency (f_p) is dependent on the plasma density n_e. One of the most important plasma parameters is plasma frequency [9]. Debye length is the important function of plasma. The distance is reflecting the charged particle which is going to impact the individual particle. It brings a reverse charge within the plasma medium. The Debye length λ_D is proportional and equivalent to the square root of the temperature T_D of the electron and inversely to the density n_D of the electron according to the Electron mass m_e, ε_o the permittivity and e the Electron charge[10].

$$\lambda_D = \sqrt{\frac{\varepsilon o \, K_B \, Te}{ne \, q2e}} \cong 7430 * \left(\frac{T_e}{n_e}\right)^{\frac{1}{2}} = \left(\frac{\epsilon_{\cdot \circ} K_B T_e}{n_e q_e^2}\right)^{\frac{1}{2}} \qquad (5)$$

(Eq. 5) $q2_{\square}$ represents the electron charge. The number of particles in the Debye sphere is represented by N_D. It is proportionate to electron density and K_B represents the Boltzmann Constant. It also represents the second condition for plasma existence. $N_D \ggg 1$[11].

$$N_D = \frac{4}{3} \pi \lambda_D^3 \, n_e \qquad (6)$$

The Plasma parameter N_D is dependent on the plasma density n_e and Debye length $\lambda_{\square}$. Nanotechnology is an important field of modern research in the field of particle structure design, synthesis, and manipulation, ranging from approximately 1-100 nm[12].

Laser liquid ablation is shown as an alternative way to create nanoparticles that are useful in a wide range of applications. PLAL has been used to prepare nanoparticles of various kinds, such as metals, oxides, alloys, and semiconductors [13, 14]. There are several beneficial advantages of PLAL. It is a simple one-step procedure and an efficient technique for the processing of large amounts of nanoparticles suspended in liquid [9]. In an atmosphere that does not require high pressure or high temperatures, the ablation process takes place. The production method of PLAL is low-cost and has chemically simple materials that do not need a catalyst. These variables ensure the development of nanoparticles that are extremely small and clean and can have high surface activity [15].

PLAL provides a wide variety of nanoparticles, which in traditional methods are difficult to obtain. Finally, by modifying the laser physical parameters such as laser energy, wavelength, repetition rate, focusing state, pulse period, and several pulses or liquid parameters such as temperature. It provides an effective approach to regulating the size and morphology of nanoparticles [16]. The PLAL method relies primarily on the elimination by laser pulses activating the plasma of the target submerged in the liquid [17]. The Nano technique is becoming increasingly important in fields such as manufacturing, agriculture, manufacturing, microelectronics, and health care. In recent years, considerable attention has been paid to the use of nanotechnology in the area of health care. Today, many therapies require a lot of time and are often very costly. Faster and much cheaper treatments can be produced by using nanotechnology [18].

Antimicrobial metal nanoparticles, including copper and silver, have an Impact on viruses, bacteria, and other microorganisms. Silver and copper nanoparticles are of interest because of their special properties that can be integrated into antimicrobial applications, biosensor materials, composite fabrics, biosensor materials, cryogenic superconducting materials, beauty products, and electrical parts. In recent years, copper nanoparticles, especially cheap nanoparticles at the level of micro-electrical applications, have received more attention and are likely to be the newest antimicrobial agents discovered[19, 20].

Furthermore, silver has always been proven to be an excellent antimicrobial [21]. Antimicrobial nanomaterials are not supposed to produce toxic disinfections, unlike ordinary chemical disinfection. The antibacterial effects of metal nanoparticles are due to their relatively small size and large volume-to-surface area ratio, allowing direct interaction with microbial membranes and the release of metal ions [19]. Nanomaterials have been used to inhibit bacteria such as *Staphylococcus aureus*. *Staphylococcus aureus* is a widespread commensal bacterium that lives in humans and in a wide range of animal species within the nares, throat, and skin. The aureus can propagate by person-to-person contact (direct or fomite-mediated) and can be zoonotically transmitted through close contact with animals or items of animal origin, like raw meat.

It is important to consider movement within and between populations because of its frequency in different ecosystems and organisms. S. Aurus is also immune to o.ne or more antibiotic types, and the continuing propagation of methicillin-resistant S. Over the past few decades, aureus (MRSA) in both human and animal species has increased the risk of developing a resistant infection that produces More complicated and pricey rehabilitation [22]. It is a pathogen of greater concern because of its ability to cause a diverse array of life-threatening infections and its capacity to adapt fast to the different environmental conditions [23].

MATERIALS AND METHODS

The experiment is performed on solid targets for Cu and Ag by using a pulsed laser. This method has generated plasma. It is achieved using laser-induced plasma spectroscopy [LIPS]. The laboratory structure for using LIPS is shown in Figure-1 below.
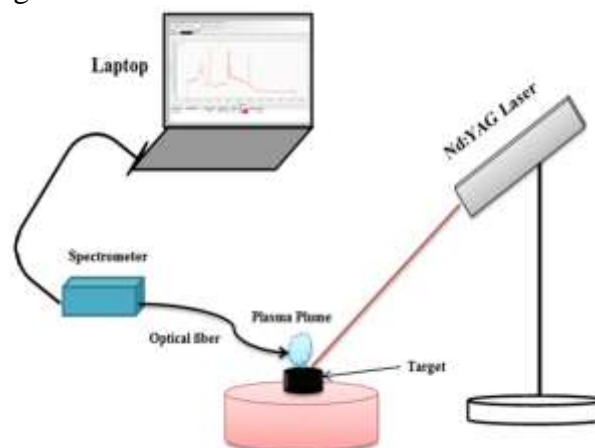
Figure 1. Laboratory arrangement for LIPS setup.

The plasma is produced in this experiment by a Q-switched pulsed laser Nd: YAG with a wavelength of (1064) nm and a frequency of 6 Hz. Q-Switch delay via laser controller is used in this phase to streak light. Pulse laser energy is transmitted by the energy meter and measured. The pulse of a laser is created by the arrangement of the operating 45^0 angles.

The laser beam hits the material which evaporates and ionizes the substance to formulate the plasma plume on the surface of the targeted material. The functional emission spectroscopy technique is used to distinguish the electron temperature, density, and frequency of this method. The spectrometer enriches this operation in each fired, spectrometers are primarily used. The Surwit [S3000-UV-NIR] spectrometer is used in this experiment to test the system's emission wavelength (200-800) and high-performance throughput.

The findings were discussed and compared with those of the National Institute of Standards and Standards Data from science (NIST database)[24]. Figure (2) shows the second experiment based on the pulsed laser ablation of the fluid method. A target of)99.99% (a pure substance (copper and silver) was placed at the bottom of a glass container containing 5 ml of distilled water, and the height of the water above the target was)14(mm. The target was irradiated by firing laser pulses to the device (Nd-YAG) of different energies (300 - 600 - 800) mJ and the number of constant pulses is (300) pulses within a short time, and the frequency of the device is constant (6) Hz

51

and the wavelength is (1064) nm. These samples were taken to the biological laboratory to study the Antibacterial effect of (Cu) (Ag) nanoparticles were carried out against the pathogenic multi-drug resistance (MDR) bacterial isolates including Gram-positive *Staphylococcus aureus* by agar well diffusion method according to the guidelines of the Clinical Laboratory Standard Institute (CLSI 2017).

The pathogenic bacterial isolates were cultured in nutrient broth for 24 hours at $37^{o}C$ and the growing cultures were diluted to the (10^{8} CFU/ml) in normal saline and spread on previously prepared Mullar-Hinton agar plates. Wells with holes of 5 mm were cut on the Mullar-Hinton agar plates, then filled with 100 μL of (Cu) (Ag) nanoparticles solution and incubated for 24 hours at $37^{o}C$ a transparent ring around the wells were measured in millimeters.
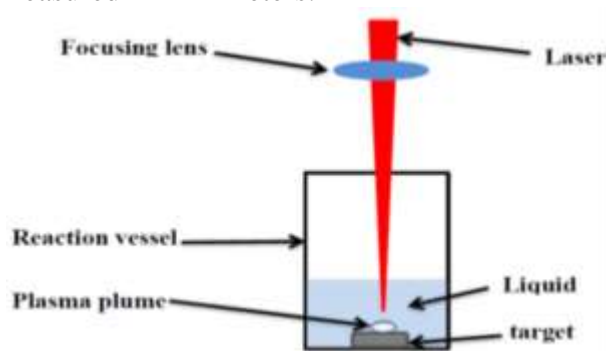
Figure 2. demonstrates the setup of PLAL technique.

RESULTS AND DISCUSSION

Influence of Laser Energy on the Emission Spectrum

The effect of pulsed laser energy on the emission spectrum of Cu and Ag plasmas at (200-800) nm wavelength range has been studied in more detail in this section.

Cu plasmas

The spectroscopic patterns formed by laser-induced tin plasma in air ambient in the range of 200 nm to 800 nm are shown in Figure -3 spectral lines in air ambient are the highest intensity lines in the plasma continuum displayed Cu spectral lines in air ambient are Cu I (at 325.42 nm), Cu I (at 465.34 nm), Cu II (at513.95nm), Cu I (at 529.44nm), Cu I (at 570.29 nm) and Cu I (at578.47nm).

Furthermore, we have reported low-intensity spectral lines such as Cu II (at 269.41 nm), Cu I (at 406.46nm), Cu I (at 427.65 nm), Cu II (at

656.35 nm), Cu II (at674.55nm), Cu II (at690.46nm), Cu II (at 777.04nm), and Cu II (at 793.01nm).

It is evident from this figure that with the growth of laser peak energy, the intensity of the spectral lines increases. This can be described as follows: Increased laser energy raises the target's average ablation rate which means that the excited atoms increase and hence increase with higher spectral strength. It can be observed from Figure -3 that laser peak energy has a strong effect on the strength of the emission lines. The strength of the spectral lines increases with the rise in the laser peak energy since the mass ablation rate of the target often increases with the increasing energy, resulting in an increase in the intensity of the spectral line. The increase in laser intensity would increase the absorption of laser energy into the plasma, resulting in greater ablation and leakage of plasma in strong alignment.
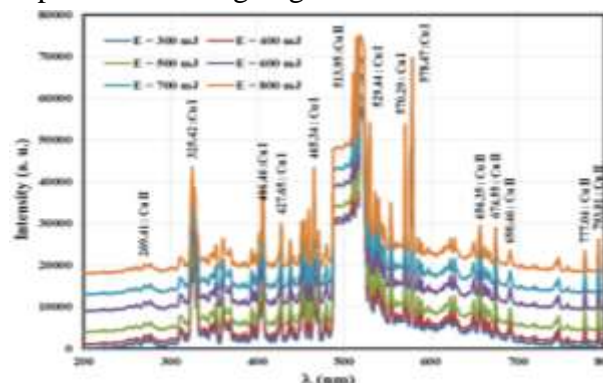
Figure 3. Emission spectra of laser-induced on pure Cu with different laser energies (300-800) mJ.

Ag plasma

The spectroscopic patterns formed by laser-induced tin plasma in air ambient in the range of 200 nm to 800 nm are shown in Figure -4 spectral lines in air ambient are the highest intensity lines in the plasma continuum displayed Ag spectral lines in air ambient are Ag I (at 518.28 nm), and AgI (at 546.07 nm).

Furthermore, we have reported low-intensity spectral lines such as Ag II (at 270.25 nm), Ag I (at 328.44nm), Ag I (at 338.83 nm), Ag II (at 421.31 nm), Ag II (at 656.59nm), and Ag II (at777.25nm). It can be observed from Figure -4 above that laser peak energy has a strong effect on the strength of the emission lines. We presume that the spectral lines' strength increases as the laser peak energy rises, since the mass ablation rate of the target also rises with increasing energy, resulting in an increase in the spectral line's

intensity. The increase in laser intensity would increase the absorption of laser energy into the plasma, resulting in greater ablation and leakage of plasma
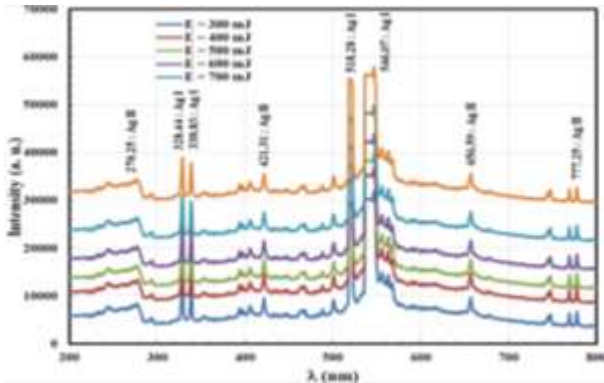
Figure 4. Emission spectra of laser-induced on pure Ag with different laser energies.

Influence of Target Metal on the Electron Temperature

For Cu and Ag plasmas, the electron temperature (T_e) emitted by lasers in the air at atmospheric pressure can be obtained from the tow line ratio equation (1).

For the calculation of the electron temperature at varying laser energies, the atomic lines of Ag I and the ionic lines of Ag II are used (300, 400,500,600,700, and 800 mJ). Table 1 and Table 2 tabulate the parameters of the Cu and Ag I spectral lines. The electron temperature was measured and plotted in Figures 4 and 5 and using the data tabulated in Tables 1 and 2 and Eq. (1).

From these tables, several characteristics can be noted, with increasing laser intensity, the electron temperature in both plasmas increases. This activity has been related to the transfer of laser thermal energy to electron kinetic energy due to increased forward peaking of laser energy of steady laser spot size [25].

Under the same terms, the electron temperature value of Ag plasma is higher than that of Cu plasma. The reason for the temperature difference is the difference in ionization energies. A target plate of copper and silver was placed in distilled water and exposed to a laser beam Nd: YAG laser of different energies causes irradiation of the metal surface (copper, silver) to excise the confined spot by laser.

Influence of Target Metal on the Electron Density

The effect of laser energy on the electron density of Ag and Cu targets is measured and plotted in Figures 5 and 6, according to equations (2). Tables 1 and 2. This figure shows that the number of electrons is inversely associated with the ionization energy of metal targets.

Table 1. Spectroscopic parameters of plasma Cu at different energies (300-800) mJ.

Laser Enerjy (mj)	T_e (eV)	$n_e * 10^{20}$ (cm^{-3})	f_p (Hz)$* 10^{14}$	$\lambda_D * 10^{-6}$ (cm)	$N_d * 10^5$
300	1.630	2.1	1.312	6.996	3.059
400	1.862	4.6	1.924	5.098	2.546
500	1.873	4.7	1.954	5.032	2.528
600	1.888	5.0	1.998	4.941	2.503
700	1.899	5.1	2.029	4.881	2.486
800	1.910	5.3	2.062	4.817	2.469

Table 2. Spectroscopic parameters of plasma Ag at different energies (300-800) mJ.

Laser Enerjy (mj)	T_e (eV)	$n_e * 10^{18}$ (cm^{-3})	f_p (Hz)$* 10^{12}$	$\lambda_D * 10^{-4}$ (cm)	$N_d * 10^6$
300	1.721	1.0	8.837	1.067	4.927
400	1.762	1.1	9.452	1.009	4.770
500	1.810	1.3	10.197	0.948	4.604
600	1.858	1.5	10.961	0.894	4.454
700	1.909	1.7	11.795	0.842	4.310
800	2.054	2.5	14.287	0.721	3.970
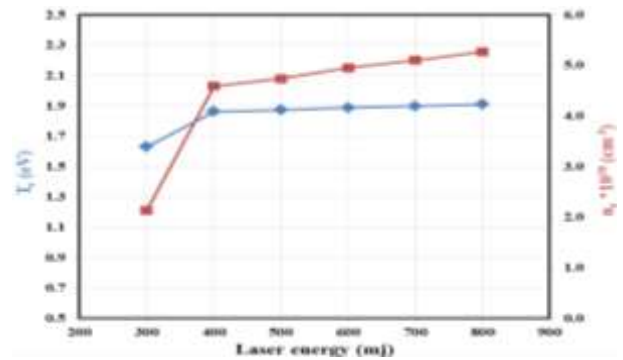
Figure 5. The variation of electron temperature and electron density with laser energy (300-800) mJ in Cu at atmospheric pressure.
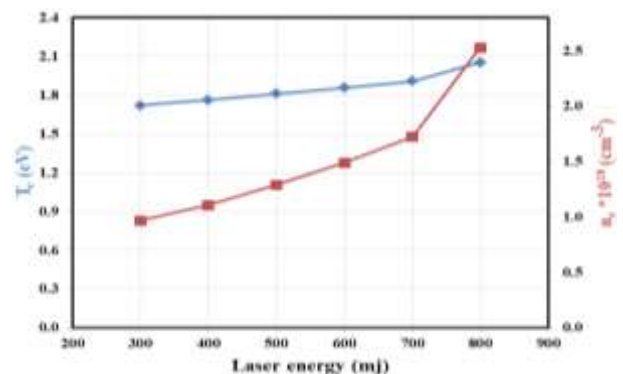
Figure 6. The variation of electron temperature and electron density with laser energy (300-800) mJ in Ag at atmospheric pressure.

53

Where the electron density of plasma would be greater for smaller metal ionization potential mainly caused by the mass ablation and consequent denser vapor plasma plume creates higher electron density. With rising laser energy, the electron density of the two-target plasma understudy is increasing. In addition, the electron density of both plasmas increases with the rise in laser radiation, depending on the ionization energy. The absorption of laser photons in plasma by electron-neutral Inverse Bremsstrahlung can be due to this rise in electron density with increased laser intensity. The excitation temperature and ionization temperature increase as the energy consumed increases, and so does the plasma's electron density.

Effect of Target Metal on the Plasma Frequency

The difference of the electron frequency with the laser energy of Ag and Cu plasmas is drawn in Figures-7 and 8 by the equation (4). Data points indicated an increase in plasma frequency with an increase in laser intensity for the two plasmas targets (Ag and Cu). This behavior is caused by an increase in the concentration of electrons, with an increase in laser intensity contributing to an increase in plasma frequency. The outcome also revealed that the plasma frequency value in Ag plasma is higher than that in Cu plasma.
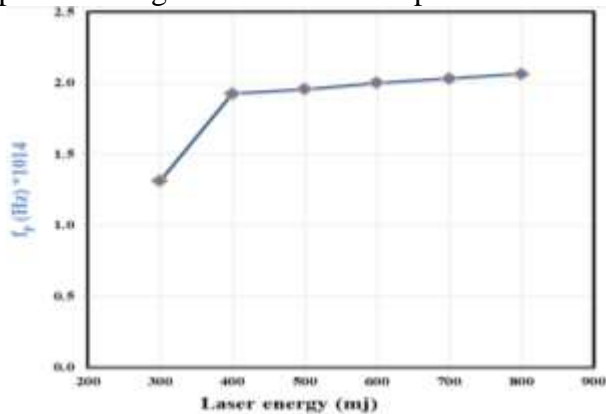
Figure 7. The plasma frequency with laser energy in Cu at (300-800) mJ.
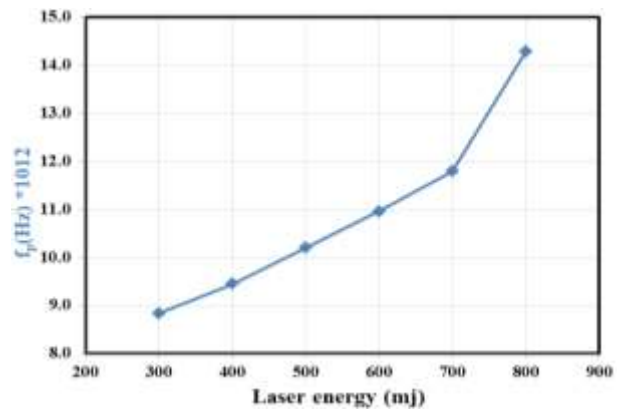
Figure 8. The plasma frequency with laser energy in Ag at (300-800) mJ.

This effect was because the concentration of electrons increased when the targets' ionization energy was reduced.

Influence of Laser energy on the Debye Length and Plasma Parameter

Debye length is a very important parameter to describe plasmas. In figures (9 and 10) explains the influence of laser energy on the duration of the Debye length and the plasma parameters measured by using equations (5) and (6), respectively. The data that were calculated were tabulated in Table-1. The findings revealed the length of Debye and plasma parameters decreased as laser energy increased. The values of Debye length and plasma parameters of Cu plasma are greater than of Ag plasma. This behavior of both parameters is attributed to the fact that the electron density increases with decreasing of the ionization energy of the target atoms.
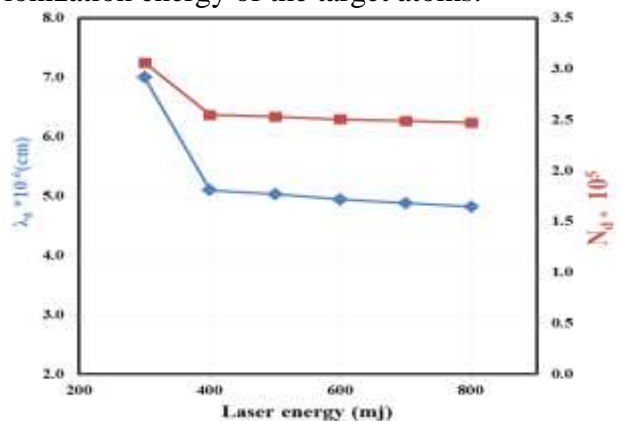
Figure 9. The Debye Length with laser energy in Cu at different energies (300-800) mJ.
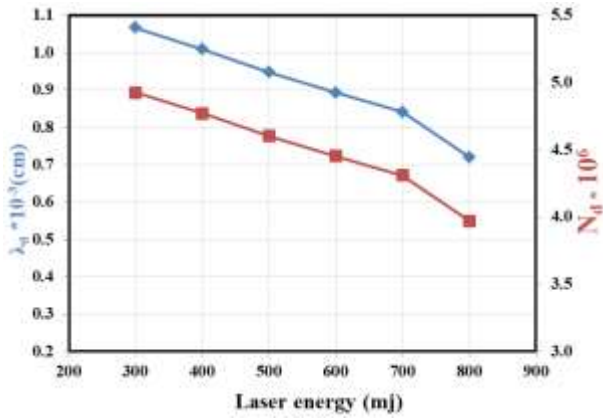
Figure 10. The Debye Length with laser energy in Ag at different energies (300-800) mj.

Silver Nanomaterial

Laser is the simplest technique for the formation of nanoparticles. The silver metal plate was irradiated with a beam of (1064) nanometers from the pulsed laser (Nd: YAG). Prepared by three samples using three different energies (300) MJ, (600) mJ, and (800) mJ, while the other parameters remained constant (p.r.r) at (6) Hz and the number of pulses was constant (300). The color of the transparent liquid (distilled water) gradually changed with the increase in the number of pulses, noting that the transparent medium may change faster with respect to the laser energy (800) mJ from the (600 and 300), as well as if the liquid changed faster at an energy (600) mJ than (300) mJ as shown in Figure 11.

Figure 11. Three samples of a Silver nanomaterial at three energies (300,600 and 800) mJ.

Copper Nanomaterial

Laser is the simplest technique for the formation of nanoparticles. The copper metal plate was irradiated with a beam of (1064) nanometers from the pulsed laser (Nd: YAG). Prepared by three samples using three different energies (300) MJ, (600) mJ, and (800) mJ, while the other parameters remained constant (P.R.R) At (6) Hz and the number of pulses was constant (300). The color of the transparent liquid (distilled water) gradually changed with the increase in the number of pulses, noting that the transparent medium may change faster with respect to the laser energy (800) mJ from the (600 and 300), as well as if the liquid changed faster at an energy (600) mJ than (300) mJ as shown in Figure 12.
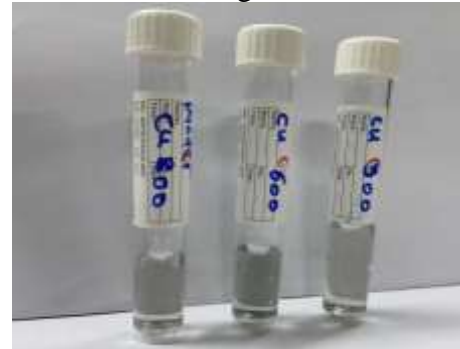
Figure 12. Three samples of Copper nanomaterial at three energies (300,600 and 800) mJ.

The Antibacterial Effect of Silver Nanoparticles

The effect of silver nanoparticles on the antibacterial activity was selected against Gram-positive *Staphylococcus aureus*. Positive results were given for all energies used in different proportions, as in Figure 13.
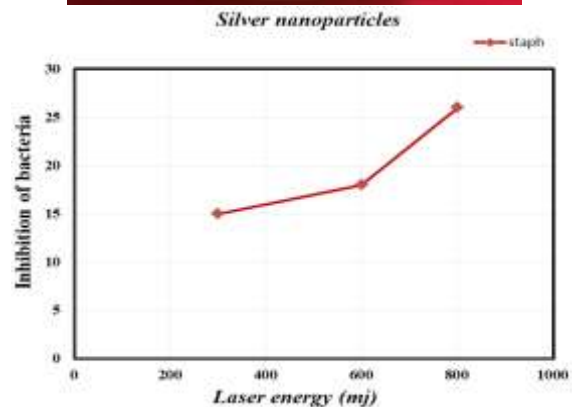
Figure 13. Image of the inhibition zone of silver nanoparticles at energies (300 - 600 - 800) mJ of *Staphylococcus aureus*.

55

The transparent ring of the inhibition zone of antimicrobial silver nanoparticles around the wells was measured in millimeters. As shown in Table 3.

Table 3. Areas of inhibition (Ag) and energies used and Nd-YAG laser characteristics.

No. of pulses	p.r.r. (Hz)	E (mj)	λ (nm)	Staphy Sample No. (mm)
300	6	300	1064	15
300	6	600	1064	18
300	6	800	1064	26

The Antibacterial Effect of Copper Nanoparticles

The effect of copper nanoparticles on the antibacterial activity was selected against Gram-positive *Staphylococcus aureus*. Positive results were given for all energies used in different proportions, as in Figure 14.
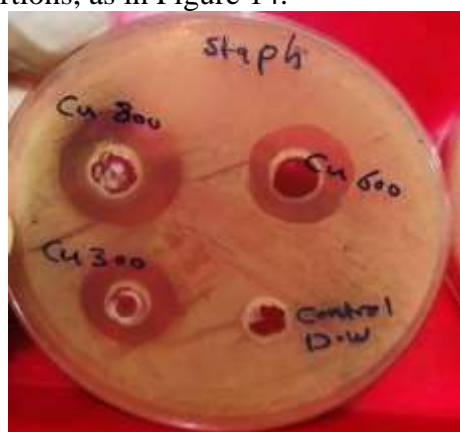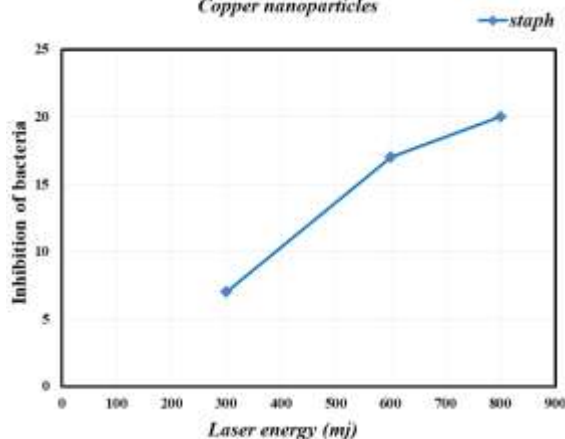
Figure 14. : Image of the inhibition zone of copper nanoparticles at energies (300 - 600 - 800) mJ of *Staphylococcus aureus*.

The transparent ring of the inhibition zone of antimicrobial copper nanoparticles around the wells was measured in millimeters. As shown in Table 4.

Table 4. Areas of inhibition (Cu) and energies used and Nd-YAG laser characteristics.

No. of pulses	p.r.r. (Hz)	E (mj)	λ (nm)	Staphy Sample No. (mm)
300	6	300	1064	7
300	6	600	1064	17
300	6	800	1064	20

CONCLUSIONS

The effects of laser energy and the properties of the laser target on the absorption spectrum and plasma properties of Ag and Cu plasmas have been illustrated in this review. Recent studies have shown that the increase in laser energy implies an increase in the strength of the emission line towards either target. The intensity of the atomic emission lines was even higher than that of the ionic lines. For any feature in the emission spectrum of the target, the presence of atomic and ionic emission lines depends on the ionization energy of the target atoms. Furthermore, the characteristics of the plasma depend on the ionization energy of the target element and the energy of the laser Also through this work, the difference between the electron density of Ag $(2.5*10^{18})$ (cm^{-3}) and Cu $(2.1*10^{20})$ (cm^{-3}) was observed, where the electron density is greater in Ag than Cu, as well as the difference in the electron temperature, which is directly proportional to the electron density Ag (2.054 ev) Cu (1.63 ev). The results showed that the prepared nanoparticles with high laser power (300) MJ are more efficient than other energies and that the bacterial cells treated with (Ag-Nps) and (Cu-Nps) were quickly inhibited. It multiplies against Gram-positive *Staphylococcus aureus* bacteria. Studies have shown that silver has a higher efficiency than copper in all energies used to kill bacteria and prevent their growth. As mentioned in the work of "Wajih, Zainab" [20].

REFERENCES

[1]   M. Hanif and M. Salik, "Optical emission studies of sulphur plasma using laser induced breakdown spectroscopy," *Optics and Spectroscopy,* vol. 116, no. 2, pp. 315-323, 2014/02/01 2014.

[2]   S. S. Harilal, B. O'Shay, M. S. Tillack, and M. V. Mathew, "Spectroscopic characterization of laser-induced tin plasma," *Journal of Applied Physics,* vol. 98, no. 1, p. 013306, 2005.

[3]   A. Safeen, W. Shah, R. Khan, A. Shakeel, Y. Iqbal, G. Asghar, R. Khan, G. Khan, K. Safeen, and W. Shah, "Measurement of plasma parameters for copper using laser induced breakdown spectroscopy," *Digest*

Journal of Nanomaterials and Biostructures, vol. 14, no. 1, pp. 29-35, 2019.

[4] L. Liliana Patricia Vera, P.-T. Jaime Andrés, and L. Henry Riascos, "Spectroscopic analysis of coal plasma emission produced by laser ablation," *Revista Facultad de Ingeniería Universidad de Antioquia,* vol. 0, no. 78, 03/18 2016.

[5] V. K. Unnikrishnan, K. Alti, V. B. Kartha, C. Santhosh, G. P. Gupta, and B. M. Suri, "Measurements of plasma temperature and electron density in laser-induced copper plasma by time-resolved spectroscopy of neutral atom and ion emissions," *Pramana,* vol. 74, no. 6, pp. 983-993, 2010/06/01 2010.

[6] M. A. Khalaf, B. M. Ahmed, and K. A. Aadim, "Spectroscopic Analysis of CdO1-X: SnX Plasma Produced by Nd: YAG Laser," *Iraqi Journal of Science,* pp. 1665-1671, 2020.

[7] S. S. Harilal, C. V. Bindhu, R. C. Issac, V. P. N. Nampoori, and C. P. G. Vallabhan, "Electron density and temperature measurements in a laser produced carbon plasma," *Journal of Applied Physics,* vol. 82, no. 5, pp. 2140-2146, 1997.

[8] Q. A. Abbas, "Effect of Target properties on the Plasma Characteristics that produced by Laser at Atmospheric Pressure," *Iraqi Journal of Science,* pp. 1251-1258, 2019.

[9] P. V. Kazakevich, A. V. Simakin, V. V. Voronov, and G. A. Shafeev, "Laser induced synthesis of nanoparticles in liquids," *Applied Surface Science,* vol. 252, no. 13, pp. 4373-4380, 2006/04/30/ 2006.

[10] T. Hameed and S. Kadhem, "Plasma diagnostic of gliding arc discharge at atmospheric pressure," *Iraqi Journal of Science,* pp. 2649-2655, 2019.

[11] B. M. Ahmed, K. A. Aadim, and M. A. Khalaf, "Verify the plasma parameters generated from the Tin material using the laser-induced plasma technique," *World Scientific News,* vol. 144, pp. 326-337, 2020.

[12] N. Iki, "Silver Nanoparticles," *Analytical Sciences,* vol. 34, no. 11, pp. 1223-1224, 2018.

[13] M. Kim, S. Osone, T. Kim, H. Higashi, and T. Seto, "Synthesis of Nanoparticles by Laser Ablation: A Review," *KONA Powder and Particle Journal,* vol. 34, pp. 80-90, 2017.

[14] A. Singh, J. Vihinen, E. Frankberg, L. Hyvärinen, M. Honkanen, and E. Levänen, "Pulsed Laser Ablation-Induced Green Synthesis of TiO2 Nanoparticles and Application of Novel Small Angle X-Ray Scattering Technique for Nanoparticle Size and Size Distribution Analysis," *Nanoscale Research Letters,* vol. 11, no. 1, p. 447, 2016/10/05 2016.

[15] J. Xiao, P. Liu, C. X. Wang, and G. W. Yang, "External field-assisted laser ablation in liquid: An efficient strategy for nanocrystal synthesis and nanostructure assembly," *Progress in Materials Science,* vol. 87, pp. 140-220, 2017/06/01/ 2017.

[16] H. J. Rafal, "Effect of (Mn , Zn and Se) Nanoparticles Synthesized in Liquid by Laser Induce Plasma on Thyroid," MSc, Physics Dept./College of Science University of Baghdad, 2020.

[17] V. Amendola and M. Meneghetti, "What controls the composition and the structure of nanomaterials generated by laser ablation in liquid solution?," *Physical Chemistry Chemical Physics,* 10.1039/C2CP42895D vol. 15, no. 9, pp. 3027-3046, 2013.

[18] R. Jin, Y. Cao, C. A. Mirkin, K. L. Kelly, G. C. Schatz, and J. Zheng, "Photoinduced conversion of silver nanospheres to nanoprisms," *science,* vol. 294, no. 5548, pp. 1901-1903, 2001.

[19] A. Fariba, G. E. Bahram, K. Farrokh, S. Tabrizy, and S. S. Pooneh, "An investigation of the effect of copper oxide and silver nanoparticles on E. coli genome by RAPD molecular markers," *J Adv Biotechnol Microbiol,* vol. 1, pp. 1-6, 2016.

[20] Z. A. Wajih and Z. T. Al-dahan, "Antimicrobial Effects of Silver Nanoparticles Produced by Laser Ablation," *Iraqi Journal of Science,* vol. 56, no. 3B, 2015.

[21] Q. H. Tran and A.-T. Le, "Corrigendum: Silver nanoparticles: synthesis, properties, toxicology, applications and perspectives (Adv. Nat. Sci: Nanosci. Nanotechnol. 4 033001)," *Advances in Natural Sciences: Nanoscience and Nanotechnology,* vol. 9, no. 4, p. 049501, 2018.

[22] C. J. Heaton, G. R. Gerbig, L. D. Sensius, V. Patel, and T. C. Smith, "Staphylococcus aureus Epidemiology in Wildlife: A Systematic Review," *Antibiotics,* vol. 9, no. 2, p. 89, 2020.

[23] A. Onanuga and T. C. Temedie, "Multidrug-resistant intestinal Staphylococcus aureus among self-medicated healthy adults in Amassoma, South-South, Nigeria," *Journal of health, population, and Nutrition,* vol. 29, no. 5, p. 446, 2011.

[24] A. Kramida, Y. Ralchenko, and J. Reader, "NIST atomic spectra database (ver. 5.3)," ed, 2015.

[25] J. Haverkamp, R. M. Mayo, M. A. Bourham, J. Narayan, C. Jin, and G. Duscher, "Plasma plume characteristics and properties of pulsed laser deposited diamond-like carbon films," *Journal of Applied Physics,* vol. 93, no. 6, pp. 3627-3634, 2003.